Available online at www.sciencedirect.com
ScienceDirect
Journal of Magnetism and Magnetic Materials 320 (2008) 575–578
Journal of magnetism and magnetic materials
www.elsevier.com/locate/jmmm

Preparation of cobalt nanoparticles from [bis(salicylidene)cobalt(II)]–oleylamine complex by thermal decomposition

Masoud Salavati-Niasari[a,b,*], Fatemeh Davar[b], Mehdi Mazaheri[c], Maryam Shaterian[b]

[a]*Institute of Nano Science and Nano Technology, University of Kashan, Kashan, P.O. Box 87317-51167, Iran*
[b]*Department of Chemistry, University of Kashan, Kashan, P.O. Box 87317-51167, Iran*
[c]*Materials and Energy Research Center, P.O. Box 14155-4777, Tehran, Iran*

Received 25 April 2007; received in revised form 17 June 2007
Available online 2 August 2007

Abstract

[Bis(salicylidene)cobalt(II)] was used as a precursor to prepare cobalt nanoparticles of average diameter 25–35 nm by thermal decomposition. The different combinations of triphenylphosphine and oleylamine were added as surfactants to control the particle size. The resultant samples are characterized by X-ray diffractometer (XRD) and transmission electron microscope (TEM) to depict the phase and morphology. The hysteresis loops of the obtained samples reveal the soft magnet behaviors the enhanced coercivity (H_c) and decreased saturation magnetization (M_s) in contrast to their respective bulk materials.

Keywords: Thermal decomposition; Cobalt; Nanoparticle; Complex

1. Introduction

Metal particles smaller than 100 nm in primary particle diameter are generally considered as nanoparticles. Such metal nanoparticles often exhibit very interesting electronic, magnetic, optical, and chemical properties. For example, their high surface-to-volume ratios have large fractions of metal atoms at surface available for catalysis [1,2]. In the case of cobalt nanoparticles, they are expected to possess exceptionally high-density magnetic property, sintering reactivity, hardness levels, excellent impact resistance properties, etc. Many studies on synthesis and magnetic properties of nanoscale metal particles and composites have been reported [3–6]. But, so far, in the literature there is no work reporting on synthesis of cobalt nanoparticles by thermal decomposition reaction by using cobalt coordination compounds. The preparation of metal particles by thermal decomposition of complexes becomes increasingly important mainly due to the easy control of process conditions, particle size, particle crystal structure, and purity [7]. Saeki et al. [8] prepared cobalt particles from the cobalt(II) chloride both by gas–solid reaction and by gas–gas reaction. They found that the hexagonal crystal-structured Co particles of several microns in diameter were produced by the gas–solid reaction while cubic Co nanoparticles were produced by the gas–gas reaction. Also recently, these cobalt particles have been synthesized by a variety of methods including thermal decomposition [9,10], gas vapor condensation [11,12], and reduction of cobalt salt [13]. For thermal decomposition, cobalt carbonyl, $Co_2(CO)_8$, has often been used as a precursor to generate nanoparticles. However, this cobalt carbonyl is strongly toxic and relatively expensive. To avoid these disadvantages, we synthesized cobalt nanoparticles by thermal decomposition of [bis(salicylidine)cobalt(II)] ([Co(sal)$_2$]), without any additional reducing agents in this study.

---

*Corresponding author. Tel.: +98 361 5555333; fax: +98 361 5552935.
E-mail address: salavati@kashanu.ac.ir (M. Salavati-Niasari).

0304-8853/$ - see front matter © 2007 Elsevier B.V. All rights reserved.
doi:10.1016/j.jmmm.2007.07.020

2. Experimental section

2.1. Materials and physical measurements

All the chemicals were of analytical grade and were used as received without further purification. The precursor complexes—bis(salicylaldiminato)cobalt(II)—were prepared according to the procedure described previously [14]. X-ray diffractometer (XRD) patterns were recorded by a Rigaku D-max C III XRD using Ni-filtered Cu Kα radiation. Elemental analyses were carried out with Carlo ERBA model EA 1108 analyzer. Transmission electron microscopy images were obtained on a Hitachi H-800 transmission electron microscope (TEM) with an accelerating voltage of 200 kV. The magnetic measurement was carried out in a vibrating sample magnetometer (VSM) (BHV-55, Riken, Japan) at room temperature.

2.2. Synthesis of cobalt nanoparticles

The current synthetic procedure is a modified version of the method developed by Hyeon and co-workers for the synthesis of nanocrystals for metals that employs the thermal decomposition of transition metal complexes [15]. Unless otherwise noted, all reactions were carried out in a dry-argon atmosphere. The overall synthetic procedure is shown in Scheme 1. In this synthesis cobalt-metal nanoparticles were prepared by the thermal decomposition of $[Co(sal)_2]$–oleylamine complex. First, the $[Co(sal)_2]$–oleylamine complex was prepared by reaction 0.6 g of $[Co(sal)_2]$ and 2 ml of oleylamine. The mixed solution was placed in a 50 ml three-neck distillation flask and heated up to 100 °C for 90 min. During all the experimental processes, the flask was flushed with high-purity Ar gas to avoid oxidation. The resulting metal–complex solution was injected into 5 g of triphenylphosphine at 220 °C. The color of the solution changed from orange to black, indicating that colloidal nanoparticles were generated. The black solution was aged at 210 °C for 45 min, and was then cooled to room temperature. The nanoparticles were precipitated by adding excess ethanol to the solution. The precipitated nanoparticles were retrieved by centrifugation. The yield of the overall synthesis was 70% based on the amount of $[Co(sal)_2]$. The nanoparticles could easily be re-dispersed in nonpolar organic solvents, such as hexane or toluene (Scheme 1). The synthesized particles were characterized by a TEM, an XRD, and a VSM.

3. Results and discussion

The morphology and particle size of the powder were determined by transmission electron microscopy (TEM, CM 200 FEG, Philips, the Netherlands). For preparation of the TEM sample, the powder was dispersed in high-purity ethanol via ultrasonic equipment for 2.4 ks. Fig. 1 shows the TEM images of cobalt powders produced at the conditions described. The morphology of cobalt particles was spherical in shape, primary particles seemed to be single crystals of nearly uniform size, and the directional linkage of particles due to magnetic interaction between particles was observed. It is observed that particles have a size ranging from 25 to 35 nm and were also mainly round in shape.

The X-ray diffraction patterns of the nanoparticle powders were collected with a Philips X'Pert, Netherlands, diffractometer equipped with a Cu Kα radiation source. The XRD pattern of fresh cobalt nanoparticles less than 30 nm in size Fig. 2(a), shows the cubic structure of cobalt. It is well known that nanometer-sized cobalt is easy to be oxidized in air. However, from XRD pattern, except for pure cubic cobalt, no other cobalt oxide phases were detected, which might result from the protection of oleate on the surface of nanoparticles. The diffraction peaks are clearly broadened, which can be the result of the reduced

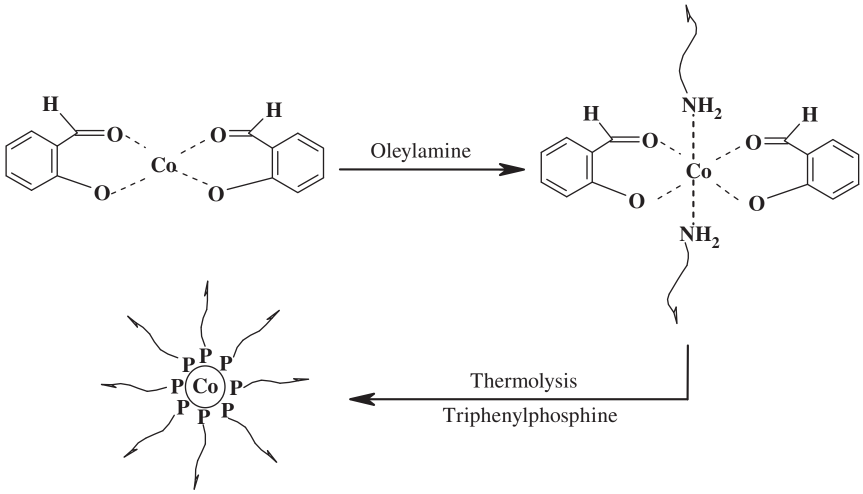

Scheme 1.

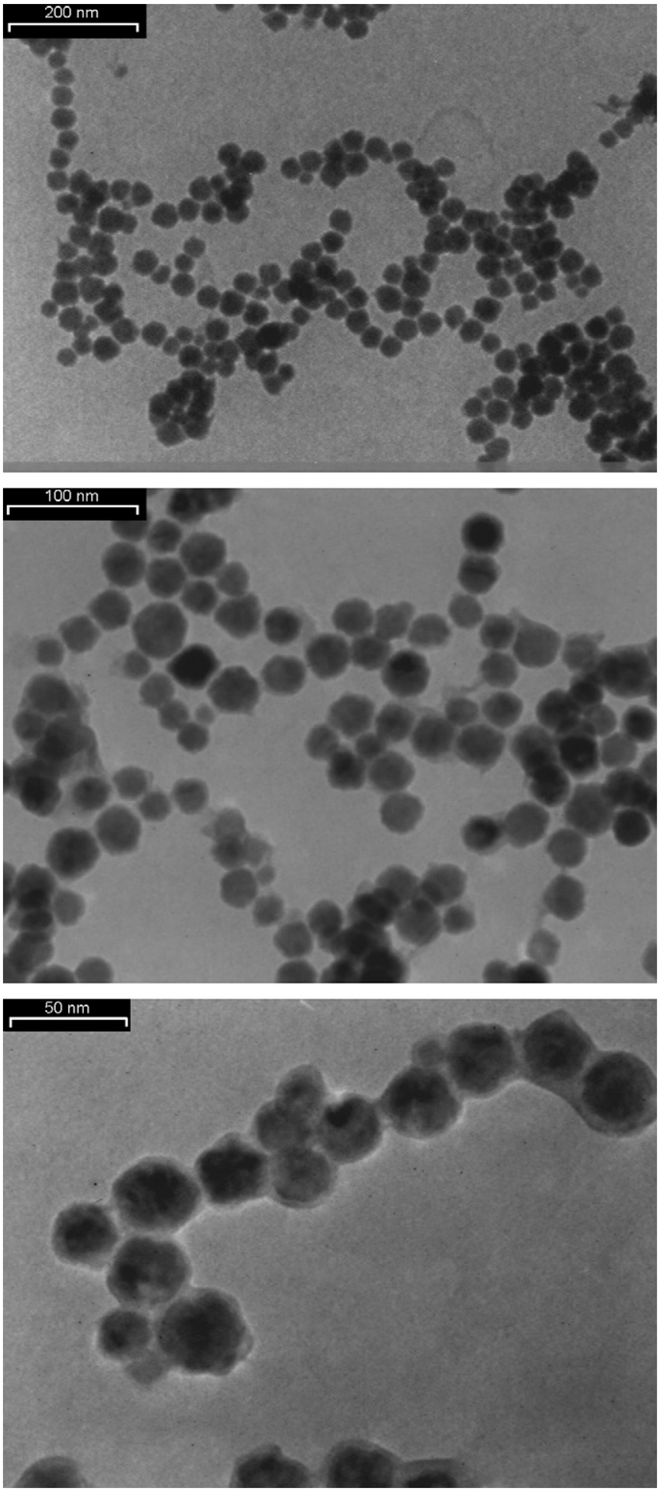

Fig. 1. TEM images of cobalt nanoparticles coated with TPP and oleylamine.

particle size. This indicates that cobalt is all nanoparticle. While the diffractogram shown in Fig. 2(b) presents the XRD pattern of nanoparticles after exposing the nanoparticles to air, no peak was related to the cobalt element in the XRD patterns. As the XRD pattern shown in Fig. 2(b) exhibits strong peaks for CoO in comparison with weak

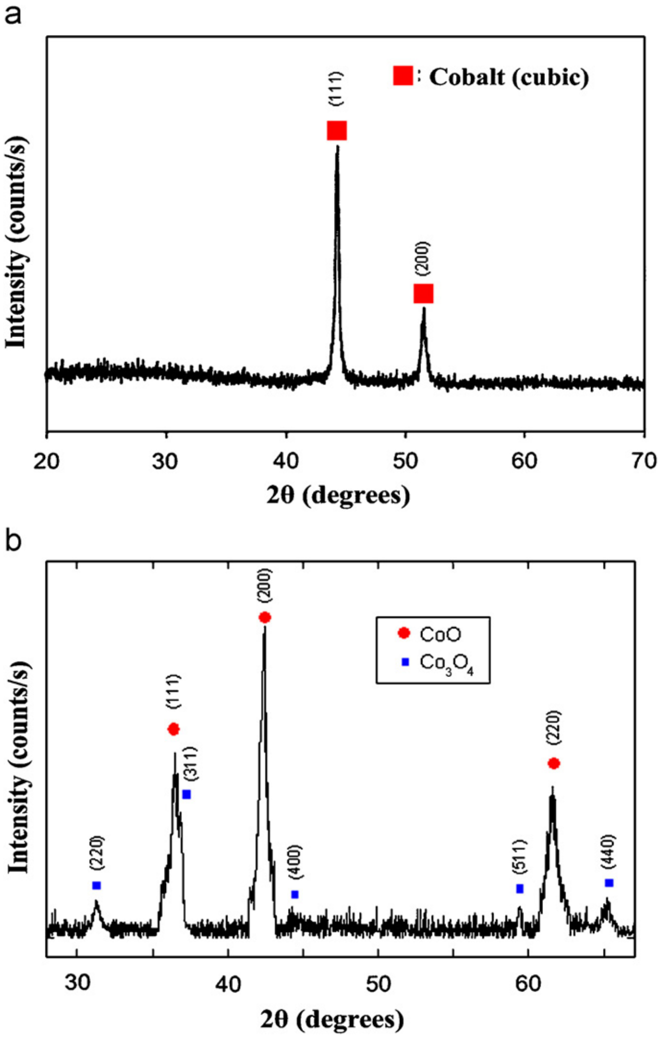

Fig. 2. X-ray diffraction pattern of (a) nanometer sized fresh Co nanoparticles and (b) nanometer sized nanoparticles after air exposure.

Co_3O_4 peaks represented by the pattern, these diffractograms show that the initially synthesized metallic cobalt nanoparticles were oxidized to CoO and Co_3O_4 nanoparticles. Using the Scherrer formula, based on line broadening, the mean crystallite sizes of the CoO and Co_3O_4 powders were determined to be 19.8 and 21.2 nm, respectively. Particles of the powder with a larger size obtained from TEM (25–35 nm) in comparison with their crystallite nanometer size (CoO: 21.2 and Co_3O_4: 16.8) are due to the polycrystalline nature of the powders.

The presence of triphenylphospine led the particles to be well dispersed with no agglomeration, while much larger particles flocculating together were synthesized in the absence of triphenylphospine. Triphenylphosphine is a high-boiling point surfactant with a patulous long-chain structure providing greater steric hindrance. So, this agent might slow the addition rate of materials to the nanoparticles during their growth, resulting in much smaller nanoparticles. Furthermore, the surfactants in the solution coordinated onto the metal of the nanoparticles, providing a dynamic organic structure that stabilizes the nanoparticles

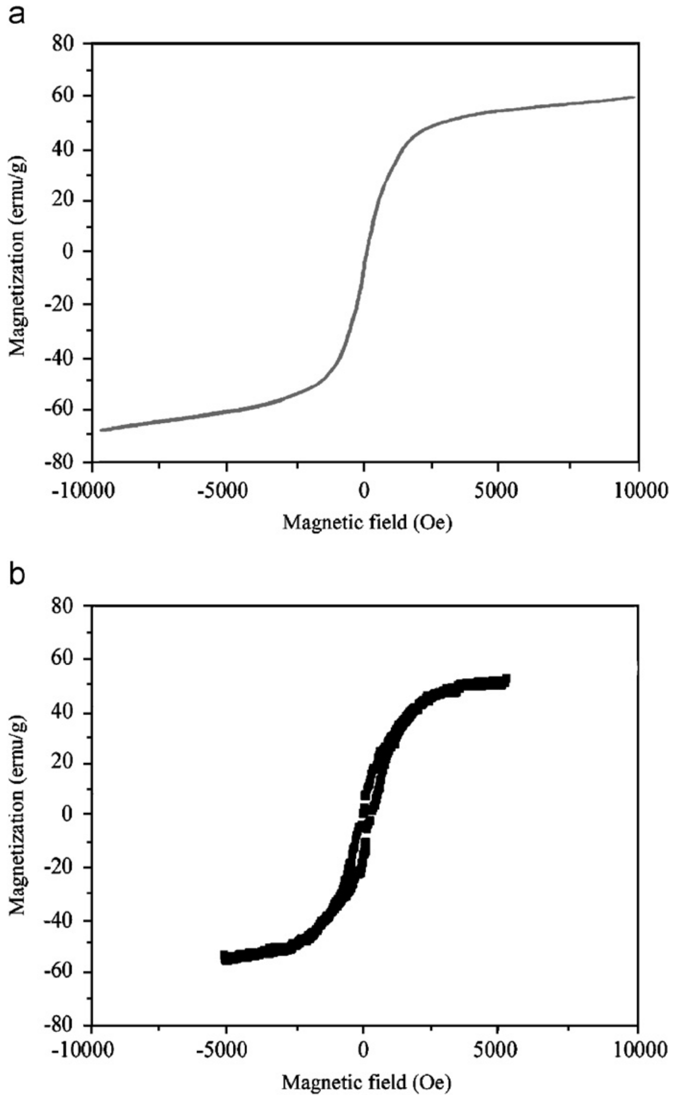

Fig. 3. Magnetization versus applied at 300 K for (a) fresh cobalt nanoparticles and (b) nanometer sized nanoparticle after air exposure.

in solution. The addition of TPP into the mixture of oleylamine and complex as an additional surfactant reduced the particle size much further and resulted in very uniform size distribution (Fig. 2). Oleylamine is known as a ligand that binds tightly to the metal nanoparticles surface. The combined effects of TPP and oleylamine were much more profound than those of individual contributions.

The soft magnet is documented by the hysteresis loop measured at 300 K as shown in Fig. 3(a). This is almost immeasurable coercively for cobalt nanoparticles at room temperature, which is a very typical behavior for a soft magnet. This indicates that the cobalt particles are soft magnets and nanosized. The saturation magnetization value, M_s, obtained by extrapolation seem to reach a maximum of around 64.1 emu/g for cobalt nanoparticles, which is lower than that of bulk cobalt particles ($M_{\mathrm{bulk}} =$ 166 emu/g) [16]. M_s decreased from 166 emu/g (for bulk cobalt) to about 64.1 emu/g (for cobalt nanoparticle). Decrease was also observed in M_s after exposing to air (Fig. 3(b)). The hysteresis loop at cobalt oxide nanoparticles exhibits a ferromagnetic behavior with M_s about 56.2 emu/g. Obviously, the coercivity (H_c) of the cobalt nanoparticles after exposing to air is enhanced while the saturation magnetization (M_s) is decreased in contrast to those of the bulk cobalt (166 emu/g and a few tens of Oersteds). These results indicate that, in spite of decrease in saturation magnetization, coercivity increases [17].

4. Conclusions

Cobalt nanoparticles have been prepared using thermal decomposition of [bis(salicylidene)cobalt(II)] in the presence of TPP and oleylamine. The as-synthesized cobalt particles show fairly good cubic cobalt crystallinity and are stable in hydrocarbon solvents against air oxidation. Compared with the bulk materials, the hysteresis loops of the obtained samples reveal soft magnet behavior, enhanced coercivity (H_c), and decreased saturation magnetization (M_s). The saturation magnetization, M_s is 64.1 emu/g for cobalt nanoparticles, which is lower than that of bulk cobalt particles ($M_{\mathrm{bulk}} = 166$ emu/g). Meanwhile, the hysteresis loop of Co nanoparticles after exposing to air also exhibits a ferromagnetic behavior with saturation magnetization (M_s) and coercivity (H_c) values of about 56.2 emu/g.

Acknowledgment

Authors are grateful to Council of University of Kashan for providing financial support to undertake this work.

References

[1] R.W. Siegel, Annu. Rev. Mater. Sci. 21 (1991) 559.
[2] R.W. Siegel, Nanophase Materials: Synthesis, Structure, and Properties, Springer Series in Material Science, 1994, p. 65.
[3] C.P. Chen, T.H. Chang, T.F. Wang, Ceram. Int. 27 (2001) 925.
[4] H. Hori, T. Teranishi, M. Taki, S. Yamada, M. Miyake, Y. Yamamoto, J. Magn. Magn. Mater. 226–230 (2001) 1910.
[5] L.C. Varanda, M. Jafelicci Jr., G.F. Goya, J. Magn. Magn. Mater. 226 (2001) 1933.
[6] K.W. Edmonds, C. Binns, S.H. Baker, M.J. Maher, S.C. Thornton, O. Tjernberg, N.B. Brookes, J. Magn. Magn. Mater. 231 (2001) 113.
[7] A. Gurav, T. Kodas, T. Pluym, Y. Xiong, Aerosol Sci. Technol. 19 (1993) 411.
[8] Y. Saeki, R. Matsuzaki, H. Nishihara, N. Aoyama, Denki Kagaku 46 (1978) 643.
[9] V.F. Puntes, K.M. Krishnan, A.P. Alivisatos, Science 291 (2001) 2115.
[10] C.B. Murray, S. Sun, W. Gaschler, et al., IBM J. Res. Dev. 45 (2001) 47.
[11] X.L. Dong, C.J. Choi, B.K. Kim, Scr. Mater. 47 (2002) 857.
[12] Z.H. Wang, C.J. Choi, B.K. Kim, J.C. Kim, Z.D. Zhang, J. Alloys Compds. 351 (2003) 319.
[13] S. Sun, C.B. Murray, J. Appl. Phys. 85 (1999) 4325.
[14] M. Salavati-Niasari, M. Shaterian, M.R. Ganjali, P. Norouzi, J. Mol. Catal. A 261 (2007) 147.
[15] H.M. Park, E. Kang, S.U. Son, H.M. Park, M.K. Lee, J. Kim, K.W. Kim, H. Noh, J. Park, C.J. Bae, J. Park, T. Hyeon, Adv. Mater. 17 (2005) 429.
[16] E.P. Wohlfarth, in: E.P. Wohlfarth (Ed.), Ferromagnetic Materials, North-Holland, Amsterdam, 1980, p. 20.
[17] L. Zhang, D. Xue, C. Gao, J. Magn. Magn. Mater. 267 (2003) 111.